Noise resistance evaluation of spatial-field optical flow using modifying Lorentzian function

Darun Kesrarat[1], Vorapoj Patanavijit[2]

[1]Department of Information Technology, Vincent Mary School of Science and Technology, Assumption University, Bangkok, Thailand
[2]Department of Computer and Network Engineering, Vincent Mary School of Engineering, Assumption University, Bangkok, Thailand

Article Info	ABSTRACT
	This paper presents the evaluation of the modifying Lorentzian function on the spatial-field optical flow to examine the validity in the noisy domain of motion estimation. In the routine of the motion estimation, the frame's motion vector is estimated by the optical flow approach where the flow of the image's frames is caught to estimate the motion vector. Nevertheless, in the noisy domain, the preciseness of the motion vector is weakened. We operated the measurement along with several non-Gaussian noises standards through several styles of the standard image frame. The determination on error vector magnitude (EVM) was taken into account to consider the preciseness of direction and length of the motion vector (MV) in comparison with various noise resistance techniques in spatial-field optical flow approach. In the achievement results, we found that this modifying Lorentzian norm function added up in the optical flow strengthen the degree of preciseness in the estimation of the spatial-field optical flow approach in the noisy domain.

Corresponding Author:

Darun Kesrarat
Department of Information Technology, Vincent Mary School of Science and Technology
Assumption University
88 Moo 8 Bang Na-Trad Km. 26 Bangsaothong, Samuthprakarn, 10570 Bangkok, Thailand
Email: darunksr@gmail.com

1. INTRODUCTION

Over 3 decades, several operations contributed to the motion vector (MV) in advance research such as motion encoding [1], [2], movement tracking [3], picture compression [4], [5], motion compensation [6], and super-resolution reformation [7], [8]. The optical flow [9], [10] is a preferred approach to arrange the MV for them. At this point, the precision of the MV is very significant because the error in MV can lead to the overall performance of the advanced researchers who used the MV as a part of their operation. In practice, many functions in the optical flow have been proposed such phase-field approach [11], global-field approach [12], and local-field approach [13]. Nonetheless, the spatial-field approach is devoted to consider in this paper [14]. Its simplicity and accessibility to determine the MV of the spatial-field optical flow approach, these made this approach became one of the admirable approaches in optical flow that was applied to use in many advanced types of research.

However, the main weakness of the spatial-field optical flow approach is very unstable to determine the MV under the noisy domain. For the noisy domain, many alternative approaches proposed the denoise mechanism [15]-[17] in the prior stage to reduce the interference in the noisy domain. Thus, this paper targets the improvement in the stability of the MV determined by the spatial-field optical flow approach under the noisy domain. Several research works considered to strengthen the stability of the spatial-field optical flow

under the noisy domain such as median function [18] and bilateral function [19] but they still presented a high gap of unstable of MV determination.

To strengthen the degree of preciseness in the MV determination of spatial-field optical flow approach under the noisy domain, this paper proposed the modifying Lorentzian norm function [20] in accompany with spatial-field optical flow approach for MV determination. We verified the achievement through the simulation of non-Gaussian noises (salt & pepper, speckle, and poison) at different noise densities and variances. We also explored the various style of successive norm images for performance verification. Meanwhile, several noise resistance techniques in spatial-field optical flow approaches were explored for comparison where the error vector magnitude (EVM) was used as the indicator for performance verification.

The paper is formatted as follows. Section 2 specifies the spatial-field optical flow approaches and noise resistance techniques. Section 3 specifies the achievement of the noise resistance indicated by the EVM. Section 4 specifies the conclusion.

2. SPATIAL-FIELD OPTICAL FLOW APPROACHES AND NOISE RESISTANCE PROCEDURE

The spatial-field optical flow approach and the noise resistance procedures are explained in this part.

2.1. Spatial-field optical flow approach

The spatial-field optical flow (SFOF) [14] is the regular optical flow approach that is used to determine the MV by scanning the movement in every pixel. In each pixel, the neighbor area around the pixel is scanned and matched for the minimum mean fault of different with a fixed frame size by considering the value of the image intensity as shown in Figure 1. With this simple protocol of SFOF, it became an admirable approach in the optical flow because it can be adjusted the neighbor area and the matching frame size according to the specific situation. By the result of the performance observation, the SFOF presents preciseness in the MV determination. But, this simple protocol, presented weakness in noise tolerance as well. The SFOF presented very poor results under the noisy domain.
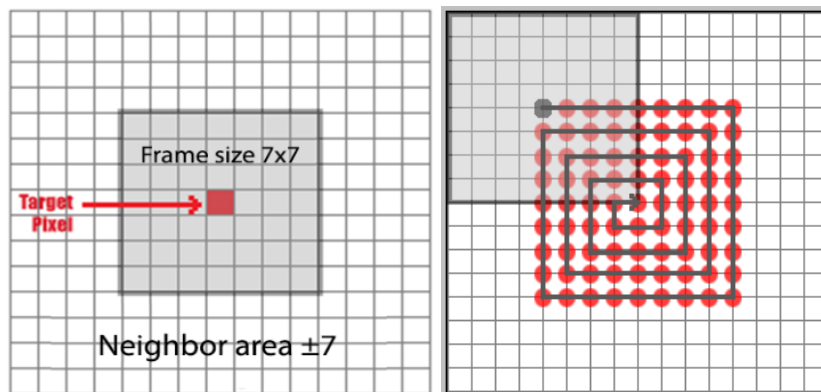

Figure 1. The neighbor area and the scanned position of the spatial-field optical flow [14]

2.2. Median function on SFOF

This is one of the approaches to strengthen the precise of the optical flow under the noisy domain. In this approach [18], the L1 median is applied in the MV of the SFOF's result. The use of L1 median [18] on SFOF (M-SFOF) is defined as:

$$(n_u, n_v) = \left(\frac{u}{|u|}, \frac{v}{|v|}\right) \tag{1}$$

where the MV (n_u, n_v) is defined by 2 scalars limit to -1, 0, and 1. The u and v are the MV from SFOF. The L1 median function, when it is applied in optical flow. It is good to apply in the area where we need to define the direction of the MV without concerning the distance of the MV. Then, it presents well noise resistance in a slow movement frame.

2.3. Bilateral function on SFOF

By traditional, the bilateral function [21] is the admirable function for noise removal that it has been applied in several areas [22]-[24]. The benefit of this bilateral function, it also has been applied in optical flow are as well. The good result in noise resistance by using the bilateral function with the SFOF. The using bilateral function [19] on SFOF (B-SFOF) is defined as:

$$v_b(x) = \frac{1}{K} \sum_{|m|<M} v(x) \emptyset(x+m) \tag{2}$$

where M is the range of neighbor vector. Here, we set M in a range of ± 7. v is the MV from SFOF. K is the normalized kernel of bilateral function. It is defined as:

$$K = \sum_{|m|<M} \emptyset(x+m) \tag{3}$$

and ϕ is a Gaussian kernel which it is defined as:

$$\emptyset(x+n) = \exp\left(\frac{|n|^2}{2\delta_a^2} + \frac{|I(x+n)-I(x)^2}{2\delta_b^2}\right) \tag{4}$$

where δ_b is the standard deviation of intensity $I(x)$. Here, we set the deviation in δ_a by $v(x) \times 7$ as the same as the primary function.

2.4. Lorentzian norm function on SFOF

This approach presented the use of modifying the Lorentzian norm function in SFOF [20]. The robust variation is the principle of problem variation in the noisy domain. To remove the noise, the Lorentzian norm function [25], [26] has been made for a robust variation area. The modifying Lorentzian norm presents more noise resistance than L1 and L2 norm. The modifying Lorentzian norm [25] is defined as:

$$P_{Lor}(x,y,s) = \log\left[1 + \frac{1}{2}\left(\frac{u(x,y,s)}{T}\right)^2\right] \tag{5}$$

for applying the modifying Lorentzian norm on the SFOF, the modifying Lorentzian norm was imposed into the influence function [21] to determine the MV and it is defined as:

$$u_{Lor}(x,y,s) = \exp\left(\frac{2 \times u(x,y,s)}{(2 \times T^2) + u(x,y,s)^2}\right) \tag{6}$$

the modifying Lorentzian norm influence is represented in quadratic where T is a set of steady thresholds as shown in Figure 2. Here, we set $T = 1.25$ as the primary function.
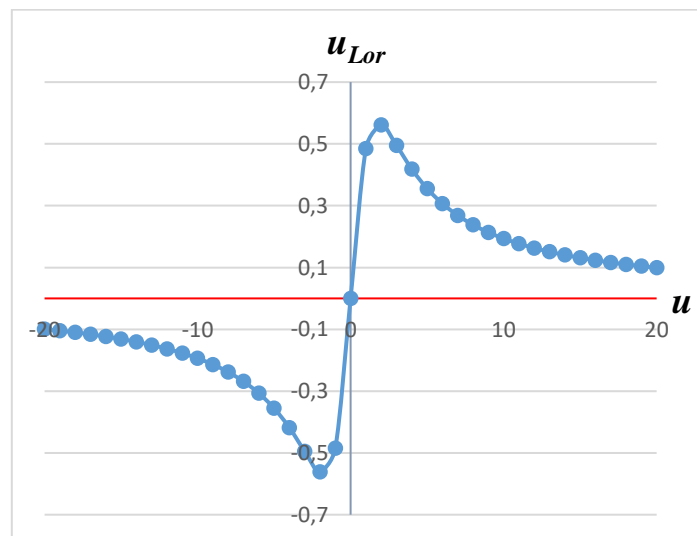

Figure 2. The modifying Lorentzian norm influence at T=1.25

3.   THE ACHIEVEMENT RESULT

The SFOF configuration in our experiment sets the neighbor area ±7 at the frame size 7x7 for each pixel. The scanning process is spiral and the closet similarity is a frame that presented the minimum mean fault different of intensity value over the scanned area. We simulated the 5 sets of non-Gaussian noises over 4 different styles of standard image frames such Akiyo, Coastguard, Container, and Foreman. The non-Gaussian noises in our experiment is shown in Figure 3 where Figure 3(a) represents non-noise, Figure 3(b) represents short noise, Figure 3(c) represents speckle @ variance 0.01, Figure 3(d) represents speckle @ variance 0.05, Figure 3(e) represents impulse @ density 0.005, and Figure 3(f) represents impulse @ density 0.025. For standard image frames, there are Akiyo, Coastguard, Container, and Foreman where 100 image frames are considered on each.

We collected the experiment result in the EVM. The strength points in evaluation by using the EVM is to measure both in direction and length of the MV where the less value close to the zero presents good noise resistance of the optical flow's result. In comparison to the performance in noise resistance, we compare the EVM value of L-SFOF against M-SFOF, B-SFOF, and SFOF. In Table 1 (see in appendix), we summarize the average EVM and SD over 100 image frames on each standard image's frame. In Figures 4-7, we report the EVM result of L-SFOF, M-SFOF, B-SFOF, and SFOF for comparison in each frame on 4 different styles of standard image frames at each set of non-Gaussian noise. Figure 4 presents EVM from coastguard image frames where Figure 4(a) represents short noise, Figure 4(b) represents speckle noise @ variance 0.01, Figure 4(c) represents speckle noise @ variance 0.05, Figure 4(d) represents impulse noise @ density 0.005, Figure 4(e) represents impulse noise @ density 0.025. Figure 5 presents EVM from Foreman image frames where Figure 5(a) represents short noise, Figure 5(b) represents speckle noise @ variance 0.01, Figure 5(c) represents speckle noise @ variance 0.05, Figure 5(d) represents impulse noise @ density 0.005, Figure 5(e) represents impulse noise @ density 0.025. Figure 6 presents EVM from Akiyo image frames where Figure 6(a) represents short noise, Figure 6(b) represents speckle noise @ variance 0.01, Figure 6(c) represents speckle noise @ variance 0.05, Figure 6(d) represents impulse noise @ density 0.005, Figure 6(e) represents impulse noise @ density 0.025. Figure 7 presents EVM from container image frames where Figure 7(a) represents short noise, Figure 7(b) represents speckle noise @ variance 0.01, Figure 7(c) represents speckle noise @ variance 0.05, Figure 7(d) represents impulse noise @ density 0.005, Figure 7(e) represents impulse noise @ density 0.025.
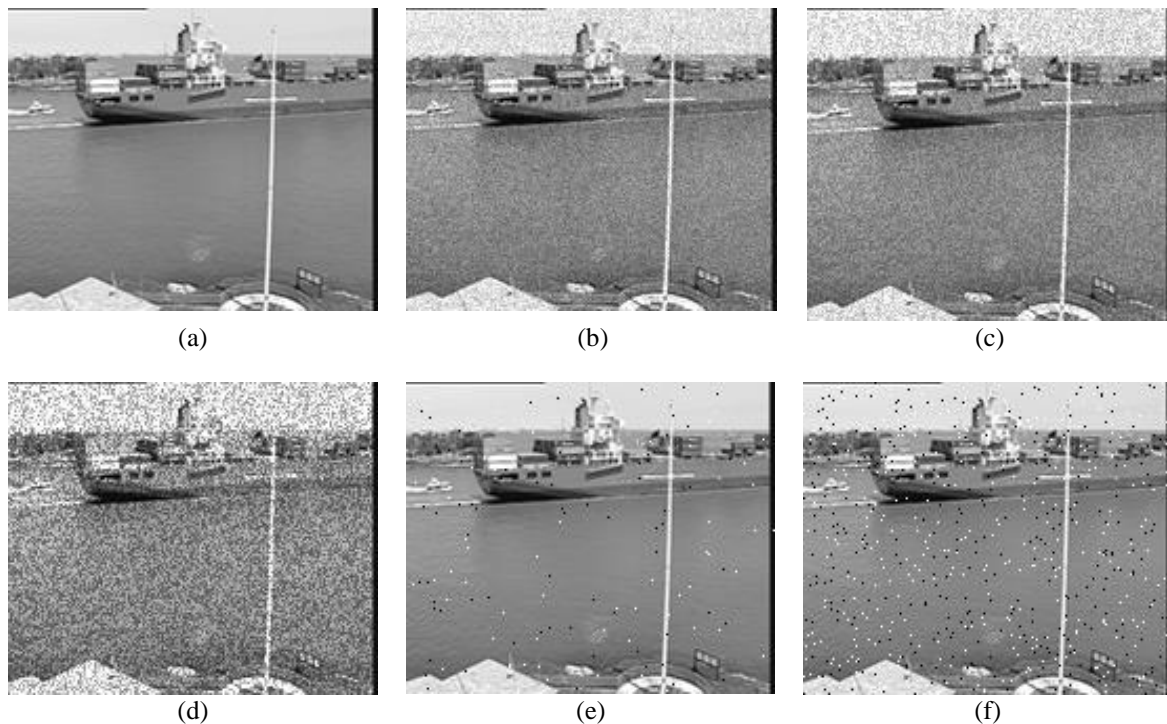

| (a) | (b) | (c) |
| (d) | (e) | (f) |

Figure 3. Non-Gaussian noises in the experiment (a) non-noise, (b) short noise, (c) speckle @ variance 0.01, (d) speckle @ variance 0.05, (e) impulse @ density 0.005, and (f) impulse @ density 0.025
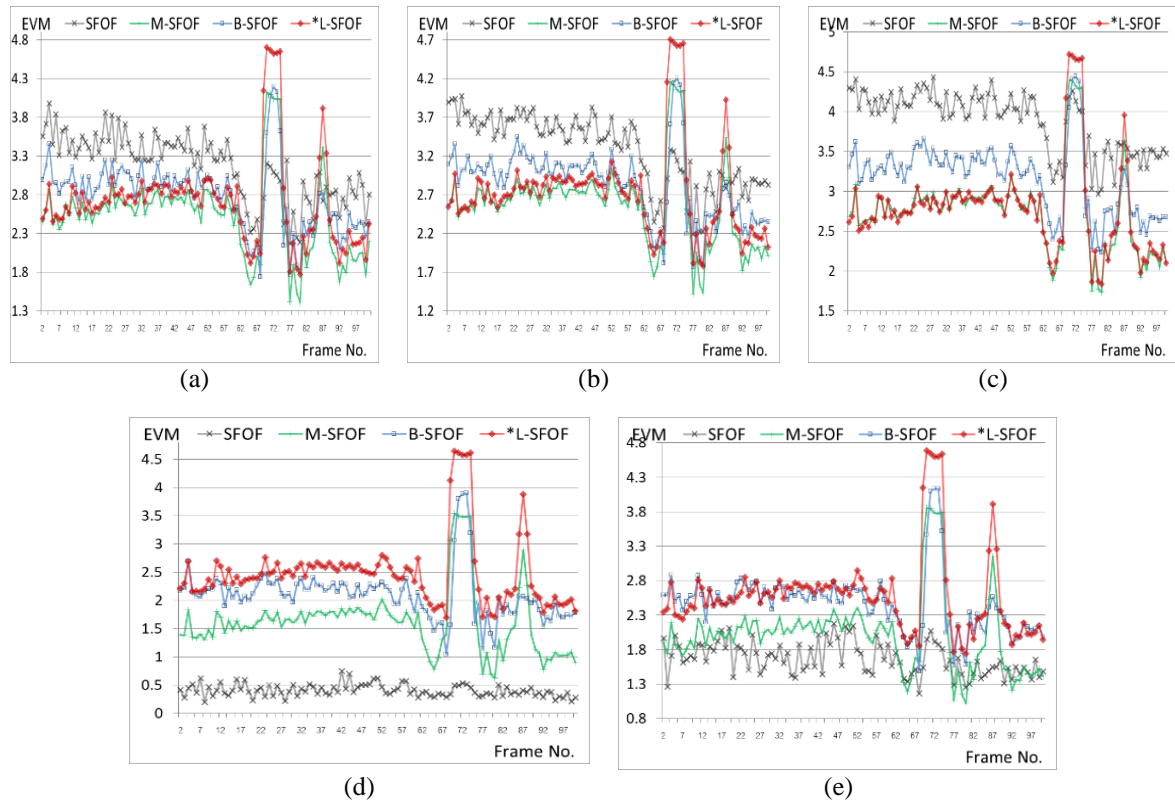
Figure 4. The achieved EVM from Coastguard (a) short noise, (b) speckle noise @ variance 0.01, (c) speckle noise @ variance 0.05, (d) impulse noise @ density 0.005, and (e) impulse noise @ density 0.025
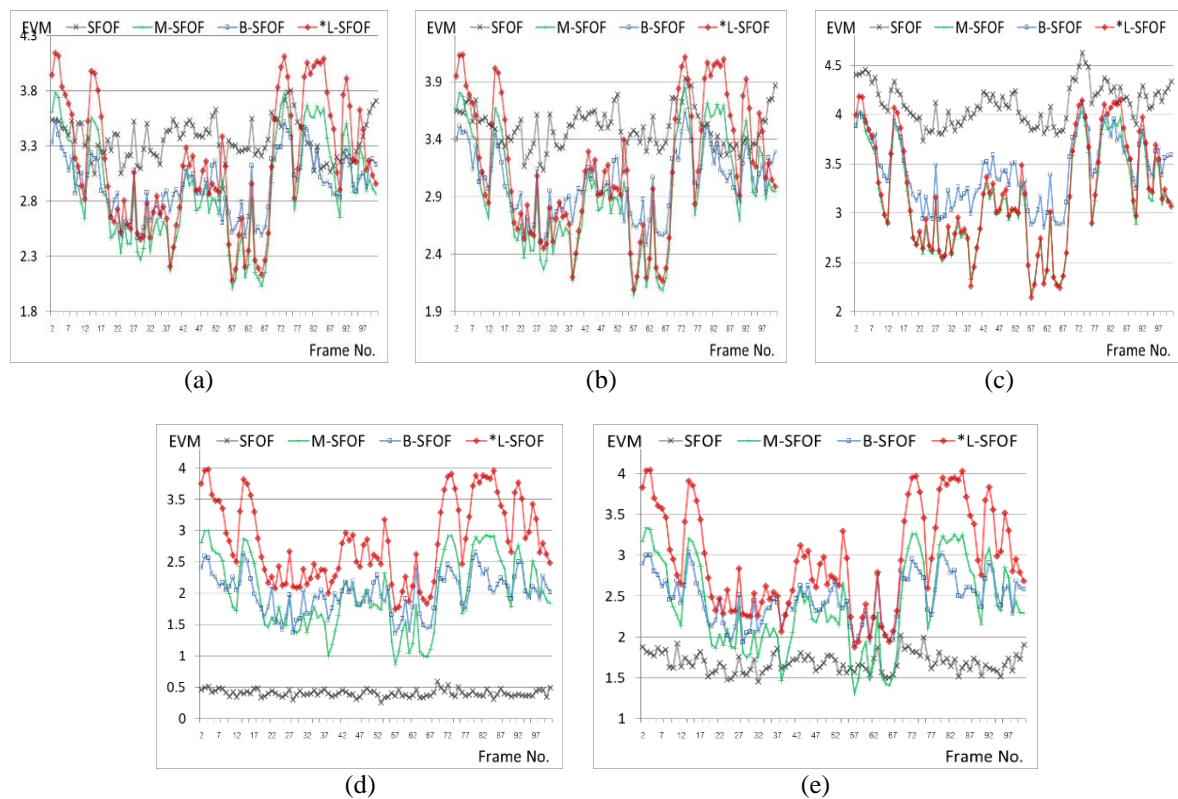

Figure 5. The achieved EVM from Foreman (a) short noise, (b) speckle noise @ variance 0.01, (c) speckle noise @ variance 0.05, (d) impulse noise @ density 0.005, and (e) impulse noise @ density 0.025
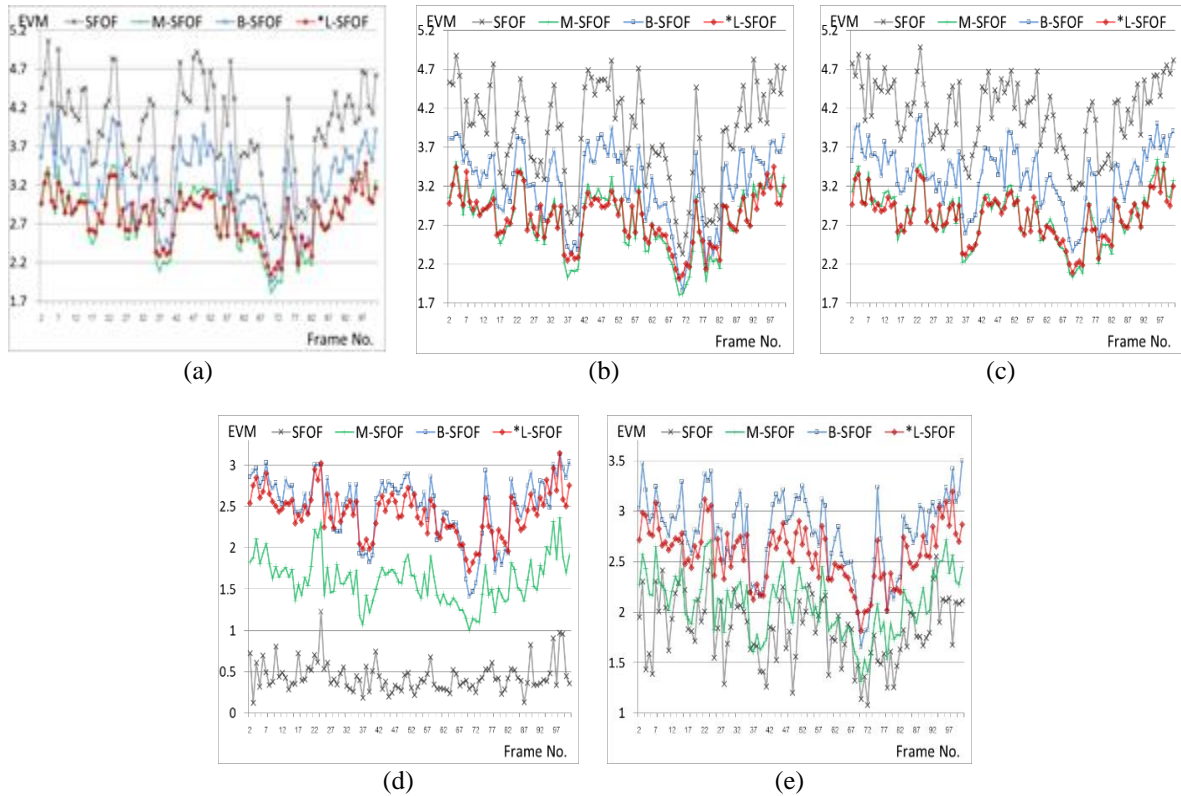
Figure 6. The achieved EVM from Akiyo (a) short noise, (b) speckle noise @ variance 0.01, (c) speckle noise @ variance 0.05, (d) impulse noise @ density 0.005, and (e) impulse noise @ density 0.025
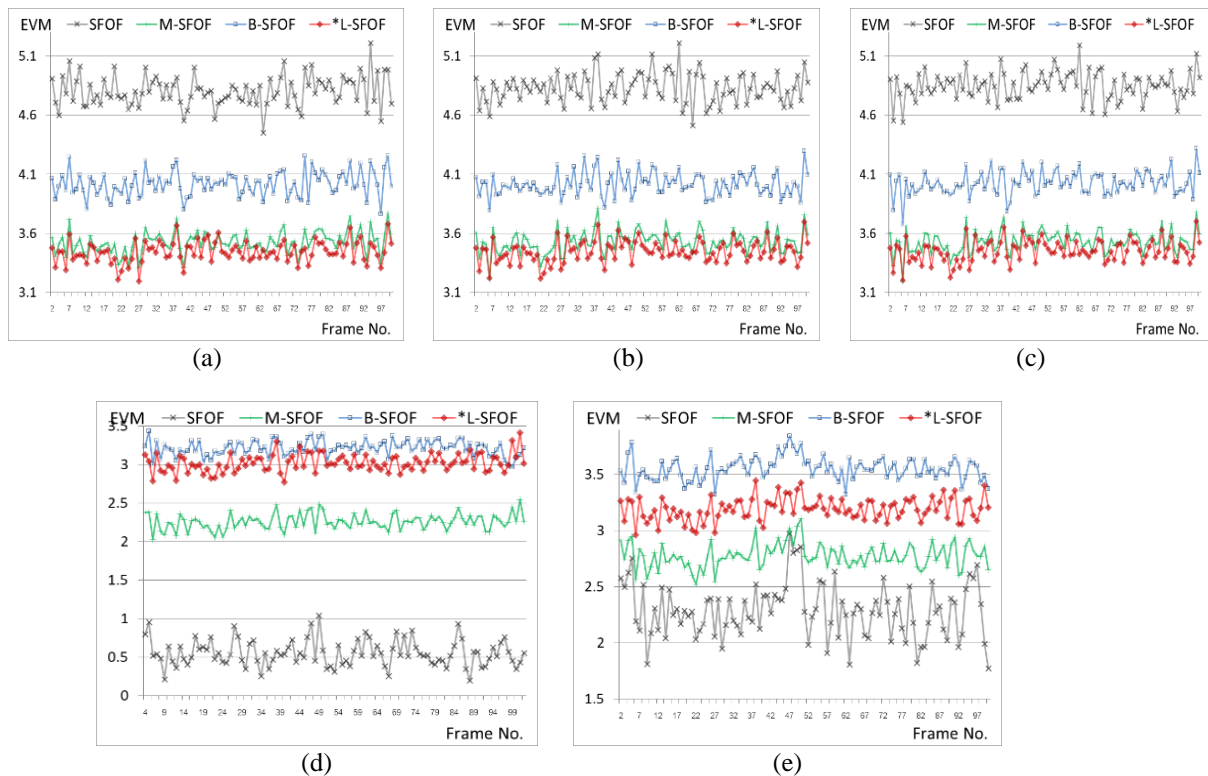

Figure 7. The achieved EVM from Container, (a) short noise, (b) speckle noise @ variance 0.01, (c) speckle noise @ variance 0.05, (d) impulse noise @ density 0.005, and (e) impulse noise @ density 0.025

4.   CONCLUSION

There are different impacts from a different set of non-Gaussian noises on SFOF in overall. The impulse noise seems less impact on SFOF where the noise resistance approaches did not help to improve the quality of MV. While the short noise and the speckle noise affected the quality of SFOF directly. The M-SFOF and the L-SFOF presented well noise resistance on the short noise and the speckle noise. When we consider the detail of the EVM result in each frame, we found that some frames M-SFOF better than L-SFOF while L-SFOF better than M-SFOF in several frames. At the same time, the level of noise also influenced the quality of the noise resistance approach. At low variance speckle noise, the M-SFOF presented better results than L-SFOF but the increasing of variance showed that the L-SFOF presented better results in Akiyo and Container with closer interval to M-SFOF in coastguard and foreman. The style of the image's frame also influences the quality of the M-SFOF and the L-SFOF. The L-SFOF always presented good results than B-SFOF in the slow movement image's frame such as Akiyo and Container. While the B-SFOF presented better than the L-SFOF result in the fast movement image's frame such coastguard and foreman on the short noise and low variance speckle noise. Then, we can consider the L-SFOF as the alternative solution in noise resistance on the short noise and the speckle noise.

APPENDIX

Table 1. The average EVM and SD

		Coastguard		Foreman		Akiyo		Container	
		AVG EVM	SD of EVM	AVG EVM	SD of EVM	AVG EVM	SD of EVM	AVG EVM	SD of EVM
Short noise	SFOF	3.163	0.426	3.353	0.177	3.890	0.626	4.803	0.130
	M-SFOF	2.532	0.535	2.904	0.485	2.760	0.400	3.523	0.094
	B-SFOF	2.792	0.453	2.947	0.268	3.216	0.508	4.019	0.107
	*L-SFOF	2.721	0.596	3.131	0.581	2.785	0.319	3.443	0.092
Impulse @d=0.005	SFOF	0.406	0.108	0.406	0.055	0.441	0.187	0.556	0.171
	M-SFOF	1.626	0.591	2.012	0.584	1.608	0.279	2.257	0.102
	B-SFOF	2.100	0.457	2.008	0.318	2.502	0.390	3.218	0.099
	*L-SFOF	2.494	0.624	2.841	0.646	2.418	0.279	3.019	0.111
Impulse @d=0.025	SFOF	1.667	0.238	1.683	0.117	1.829	0.337	2.286	0.243
	M-SFOF	2.029	0.563	2.395	0.553	2.080	0.306	2.778	0.111
	B-SFOF	2.478	0.446	2.470	0.293	2.791	0.388	3.554	0.103
	*L-SFOF	2.598	0.608	2.968	0.622	2.572	0.284	3.194	0.103
Speckle @v=0.01	SFOF	3.280	0.456	3.490	0.170	3.859	0.632	4.831	0.128
	M-SFOF	2.565	0.533	2.946	0.491	2.748	0.405	3.529	0.097
	B-SFOF	2.846	0.467	3.013	0.278	3.208	0.491	4.016	0.099
	*L-SFOF	2.733	0.594	3.144	0.580	2.780	0.330	3.447	0.094
Speckle @v=0.05	SFOF	3.886	0.376	4.109	0.197	4.142	0.438	4.850	0.119
	M-SFOF	2.747	0.529	3.144	0.517	2.820	0.348	3.531	0.095
	B-SFOF	3.171	0.443	3.429	0.337	3.336	0.395	4.024	0.100
	*L-SFOF	2.789	0.583	3.210	0.572	2.807	0.296	3.450	0.094

REFERENCES

[1] T. Wiegand, G. Sullivan, and A. Luthra, *Final draft international standard of joint video specification*, ITU-T/SG16/06, JVT-G050, 2003.
[2] M. P. E. G. Standar, *Information technology-coding of audio visual objects-part 2: visual*,'' JTC1/SC29/WG11, ISO/IEC 14 469-2 (MPEG-4 Visual)," 2000.
[3] C. S. Royden and K. D. Moore, "Use of speed cues in the detection of moving objects by moving observers," *Vision Research*, vol. 59, pp. 17–24, Apr. 2012, doi: 10.1016/j.visres.2012.02.006.
[4] Z. Chen, T. He, X. Jin, and F. Wu, "Learning for video compression," in *IEEE Transactions on Circuits and Systems for Video Technology*, vol. 30, no. 2, pp. 566–576, Feb. 2020, doi: 10.1109/TCSVT.2019.2892608.
[5] A. J. Qasim, R. Din, and F. Q. A. Alyousuf, "Review on techniques and file formats of image compression*," Bulletin of Electrical Engineering and Informatics*, vol. 9, no. 2, pp. 602-610, Apr. 2020, doi: 10.11591/eei.v9i2.2085
[6] S. A. Mahmoudi, M. Kierzynka, P. Manneback, and K. Kurowski, "Real-time motion tracking using optical flow on multiple GPUs," *Bulletin of the Polish Academy of Sciences. Technical Sciences,* vol. 62, no. 1, pp. 139-150, 2014, doi: 10.2478/bpasts-2014-0016.
[7] C. Deng, C. Deng, J. Liu, W. Tian, S. Wang, H. Zhu, and S. Zhang, "Image super-resolution reconstruction based on L1/2 sparsity," *Bulletin of Electrical Engineering and Informatics,* vol. 3, no. 3, pp. 155-160, Sep. 2014, doi: 10.11591/eei.v3i3.284.
[8] D. Kesrarat, K. Thakulsukanant, and V. Patanavijit, "A novel elementary spatial expanding scheme form on sisr method with modifying geman&mcclure function," *TELKOMNIKA (Telecommunication Computing Electronics and Control)*, vol. 17, no. 5, pp. 2554-2560, Oct. 2019, doi: 10.12928/telkomnika.v17i5.12799.

[9] A. Burton and J. Radford, *Thinking in Perspective: Critical Essays in the Study of Thought Processes*, Routledge, 1978.

[10] D. H. Warren and E. R. Strelow, *Electronic spatial sensing for the blind: contributions from perception, rehabilitation, and computer vision*, Springer Science & Business Media, vol. 99, 2013.

[11] D. J. Fleet and A. D. Jepson, "Computation of component image velocity from local phase information," *International journal of computer vision,* vol. 5, pp. 77-104, Aug. 1990, doi: 10.1007/BF00056772.

[12] B. K. P. Horn and B. G. Schunck, "Determining optical flow," *Artificial Intelligence*, vol. 17, no. 1-3, pp. 185-203, Aug. 1981, doi: 10.1016/0004-3702(81)90024-2.

[13] B. D. Lucas and T. Kanade, "An iterative image registration technique with an application to stereo vision," in *proceeding of Defense Advanced Research Projects Agency (DARPA) Image Understanding Workshop*, vol. 81, pp. 674-679, 1981.

[14] T. R. Reed, *Digital image sequence processing, compression, and analysis*, CRC press, 2004.

[15] V. Patanavijit and K. Thakulsukanant, "A computational experimental investigation of noise suppressing technique stand on hard decision threshold dissimilarity under fixed-intensity impulse noise," *Indonesian Journal of Electrical Engineering and Computer Science (IJEECS)*, vol. 23, no. 4, pp. 144-156, Oct. 2021, doi: 10.11591/ijeecs.v24.i1.pp144-156.

[16] V. Patanavijit and K. Thakulsukanant, "The novel noise classification techniques found on quadruple threshold statistical detection filter under FIIN environment," *Bulletin of Electrical Engineering and Informatics,* vol. 10, no. 5, pp. 2520-2529, Oct. 2021, doi: 10.11591/eei.v10i5.3105.

[17] L. Abderrahim, M. Salama, and D. Abdelbaki, "Novel design of a fractional wavelet and its application to image denoising, *Bulletin of Electrical Engineering and Informatics*, vol. 9, no. 1, pp. 129-140, Feb. 2020, doi: 10.11591/eei.v9i1.1548.

[18] T. Kondo and W. Kongpawechnon, "Robust motion estimation methods using gradient orientation information," *ScienceAsia,* vol. 35, no. 2, pp. 196-202, 2009, doi: 10.2306/scienceasia1513-1874.2009.35.196.

[19] D. Kesrarat and V. Patanavijit, "Noise resistance territorial intensity-based optical flow using inverse confidential technique on bilateral function," *Bulletin of Electrical Engineering and Informatics*, vol. 10, no. 6, pp. 3240-3248, Dec. 2021, doi: 10.11591/eei.v10i6.3243.

[20] D. Kesrarat and V. Patanavijit, "Robust optical flow using adaptive Lorentzian filter for image reconstruction under noisy condition," in *Proceedings of IEEE Explore of the 2016 8th International Conference on Graphic and Image Processing (ICGIP 2016)*, vol. 10225, pp. 279-284, Oct. 2016, doi: 10.1117/12.2266724.

[21] S. Paris, P. Kornprobst, J. Tumblin, and F. Durand, "Bilateral filtering: theory and applications," *Foundations and Trends in Computer Graphics and Vision*, vol. 4, no. 1, pp. 1-73, Aug 2009, doi: 10.1561/0600000020.

[22] M. G. Mozerov, "Constrained optical flow estimation as a matching problem," in *IEEE Transactions on Image Processing*, vol. 22, no. 5, pp. 2044-2055, May 2013, doi: 10.1109/TIP.2013.2244221.

[23] J. Sun, Y. Li, S. B. Kang, and Heung-Yeung Shum, "Symmetric stereo matching for occlusion handling," *2005 IEEE Computer Society Conference on Computer Vision and Pattern Recognition (CVPR'05)*, 2005, pp. 399-406 vol. 2, doi: 10.1109/CVPR.2005.337.

[24] M. Zhang and B. Gunturk, "A new image denoising method based on the bilateral filter," *2008 IEEE International Conference on Acoustics, Speech and Signal Processing*, 2008, pp. 929-932, doi: 10.1109/ICASSP.2008.4517763.

[25] P. J. Huber, "Robust statistics," *International encyclopedia of statistical science*, pp. 1248-1251, 2011, doi: 10.1007/978-3-642-04898-2_594.

[26] M. J. Black, G. Sapiro, D. H. Marimont, and D. Heeger, "Robust anisotropic diffusion," in *IEEE Transactions on Image Processing*, vol. 7, no. 3, pp. 421-432, Mar. 1998, doi: 10.1109/83.661192.

BIOGRAPHIES OF AUTHORS

Darun Kesrarat 🔟 👤 SC P received the B.S., M.S., and Ph.D. from the Department of Information Technology at Assumption University, Bangkok, Thailand. He is currently an Assistance Professor. His research areas include signal processing on image/video reconstruction, super-resolution reconstruction (SRR), motion estimation, and optical flow estimation. He can be contacted at email: darunksr@gmail.com.

Vorapoj Patanavijit 🔟 👤 SC P received the B.Eng., M.Eng., and Ph.D. degrees from the Department of Electrical Engineering at the Chulalongkorn University, Bangkok, Thailand, in 1994, 1997 and 2007 respectively. He is currently an Associate Professor. He works in the field of signal processing and multidimensional signal processing, specializing, in particular, on image/video reconstruction, super-resolution reconstruction (SRR), compressive sensing, enhancement, fusion, digital filtering, denoising, inverse problems, motion estimation, and optical flow estimation and registration. He can be contacted at email: patanavijit@yahoo.com.